

© 2021. S. Duan, X. Liu, J. Yuan, Z. Wang.

This is an open-access article distributed under the terms of the Creative Commons Attribution-NonCommercial-NoDerivatives License (CC BY-NC-ND 4.0, <https://creativecommons.org/licenses/by-nc-nd/4.0/>), which permits use, distribution, and reproduction in any medium, provided that the Article is properly cited, the use is non-commercial, and no modifications or adaptations are made.



# PSEUDO-STATIC TEST OF STEEL-GLULAM COMPOSITE BEAM-TO-COLUMN EXTERIOR JOINTS

SHAOWEI DUAN<sup>1</sup>, XINGLONG LIU<sup>2</sup>, JIAN YUAN<sup>3</sup>, ZHIFENG WANG<sup>4</sup>

Steel-glulam structure is a new type of composite structure, glulam have lateral support effect on steel plate, that can prevent premature buckling of steel plate and improve the stability of steel structure. In order to study the influence of column's cross-section form on the seismic performance of steel-glulam composite beam-to-column exterior joint, the column's cross-section form was taken as the basic variable (glulam rectangular section , H-beam section and H-beam-glulam rectangular section were used respectively). The pseudo-static tests of three composite beam-to-column joints were carried out to observe the different failure modes, and obtain the mechanical performance indexes. The experiment results demonstrated that: The energy dissipation capacity of beam-to-column exterior joint composed of glulam column was the worst, the ultimate bearing capacity and stiffness were the lowest. The ultimate bearing capacity of the exterior joints formed by the H-beam column and the H-beam-glulam composite column were both high, and their ductility coefficients were similar, while the former had better energy dissipation capacity.

*Key words:* beam-to-column exterior joint, Steel-glulam, pseudo-static test, cross-section form, energy dissipation capacity.

<sup>1</sup>Prof., PhD., Central South University of Forestry and Technology, College of Civil Engineering, Changsha, Hunan, China, e-mail: 450741204@qq.com.

<sup>2</sup>Master, Eng., Shenzhen Huayang International Design Group Co., Ltd. Changsha Branch, Changsha, Hunan, China, e-mail: 1073342372@qq.com.

<sup>3</sup>Prof., PhD., Central South University of Forestry and Technology, College of Civil Engineering, Changsha, Hunan, China, e-mail: yuanjian0571@163.com.

<sup>4</sup>Prof., PhD., Central South University of Forestry and Technology, College of Civil Engineering, Changsha, Hunan, China, e-mail: 310682339@qq.com.

## 1. INTRODUCTION

With the rapid development of the construction industry, the pollution of reinforced concrete structure building to the environment is more and more obvious. The development of green building has become an inevitable trend in the future. The timber as a traditional building material, it has many advantages: naturally renewable, low energy consumption, degradable, and low pollution. The wood structure in line with the global sustainable development strategy of building energy conservation and environmental protection[1]. At the same time, steel structures are widely used, and they are an efficient, fast, and environment-friendly building. Steel has the advantages of high strength, light weight, and good ductility, but under the same bearing capacity, the member is slender and the plate is thin, so it is prone to overall instability or local buckling under earthquakes [19]. If steel and timber are combined to form a steel-timber composite structure, the timber can play a role of lateral support to the steel plate, which can improve the stability of the steel structure and give full play to the strength of steel. At present, the international research on composite structures mainly includes steel-concrete composite structures [2,14,20,15], timber-concrete composite structures [4,21,10], and steel-timber composite structures. Among them, the research of steel-timber composite structure is still in its infancy. The related research include: the bending performance of steel-timber composite beams [3,6,12,8,17]; the experimental analysis of eccentric compression performance of steel-timber composite columns [18]; the study on the static performance of steel-timber composite connectors [9]. These tests and theoretical studies show that the mechanical properties of steel-timber composite members have higher bearing capacity and better stability than single-material members. The steel-timber composite members connected by structural glue and bolts have better synergistic mechanical properties. Hiroshi Kuramoto et al.[11] carried out an experimental study on the seismic performance of steel-concrete composite beam-to-column joints, this kind of composite beams and columns were surrounded by a layer of engineered wood. And they performed a finite element software simulation analysis. The research results show that the joint has a strong energy consumption capability. The failure modes are bending failure of beams and shear failure of joints. Nouri Farshid et al.[16] carried out an

experimental study on the shear performance and negative moment bearing capacity of steel-timber composite beam-to-column joints with shear tab. The results show that the ultimate bearing capacity and ductility coefficient of steel-timber composite beam-to-column joints with shear tab are higher than those of steel-concrete composite beam-to-column joints.

However, most of the current researches about steel-timber composite structures focus on the mechanical properties of composite beams and columns, and few studies on steel-timber composite joints. Therefore, three steel-glulam composite beam-to-column joints are designed and manufactured in this paper. The energy dissipation capacity, ductility, stiffness, and bearing capacity of the composite joints are analyzed through pseudo-static tests, and the test can provide a basis for the study about the steel-timber composite frame.

## 2. EXPERIMENTAL INVESTIGATION

### 2.1. TEST SPECIMENS

In this test, three steel-glulam composite beam-to-column exterior joint test pieces were designed and processed, presented in Fig.1(a). Each joint used the same steel-glulam composite beam, the length of the beam was 800mm and the cross-sectional dimensions were 150mm×200mm. The composite beams were made of two glulam boards with a steel plate in the middle to form a rectangular cross-section beam, and two rows of bolts were used for fastening, as shown in Fig.1(b). The cross-sections of the columns in the three steel-glulam composite beam-to-column exterior joints were different. The cross-section of the column was a rectangular section of glulam in the JT joint, the cross-section of the column was a H-beam section in the JS joint, and the cross-section of the column was a H-beam-glulam composite rectangular section in the JSTC joint. Both JS and JSTC joint used the Hot-rolled H-beam 200×200×8×6 (mm). The cross-sections of columns are shown in Fig.2. The lengths of the columns were both 1500mm, and the cross-sectional dimensions were 200mm×200mm. The steel and timber in each joint were bonded with modified epoxy resin to make the steel-glulam composite beam and column had better overall mechanical performance.

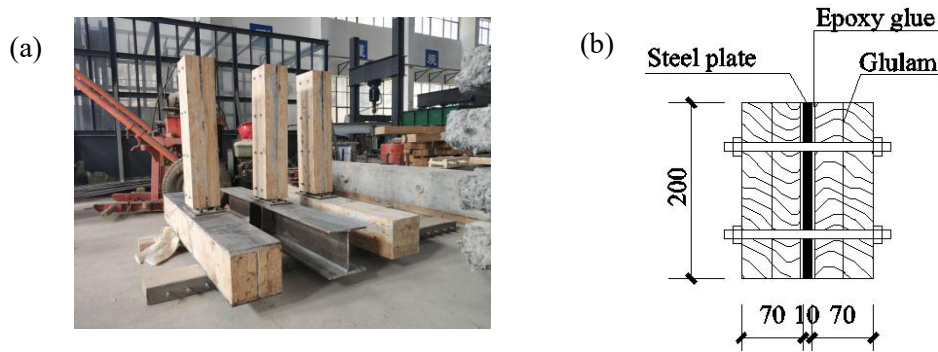


Fig.1. The photo of composite joints and Cross-section form of composite beam: (a)The photo of composite joints;(b)Cross-section form of composite beam

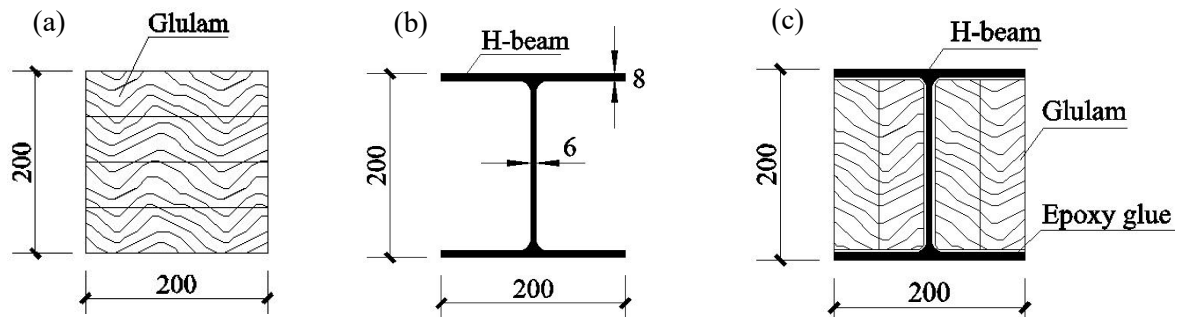


Fig.2. Cross-section form of column in each joint:(a)JT joint ;(b)JS joint;(c)JSTC joint

The steel-glulam composite beam-to-column exterior joints were all connected by welding extended end-plates and bolts, as shown in Fig.3. The steel plate, the end-plate and the H-beam were all made of Q235 steel, and the timber was made of larch. The thickness of the steel plate in the steel-glulam composite beam and the welded end-plate at the beam end were both 10mm. The core area of JS joint was welded with 4 stiffeners, as shown in Fig.3(b). The performance grades of the fastening bolts in steel-glulam composite beams were all grade 4.8 and the diameters were  $\phi 8$ . The welded end-plates were connected to the columns by 8 bolts, the bolt performance grades were all 10.9 and the diameters were  $\phi 12$ . Considering the compressive strength of timber was much lower than that of steel, there was a gap of 20mm on the timber at one end of each steel-glulam composite beam, as shown in Fig.3(a-c).The dimensions of the welded end-plates of each joint were exactly the same,as shown in Fig. 3(d).

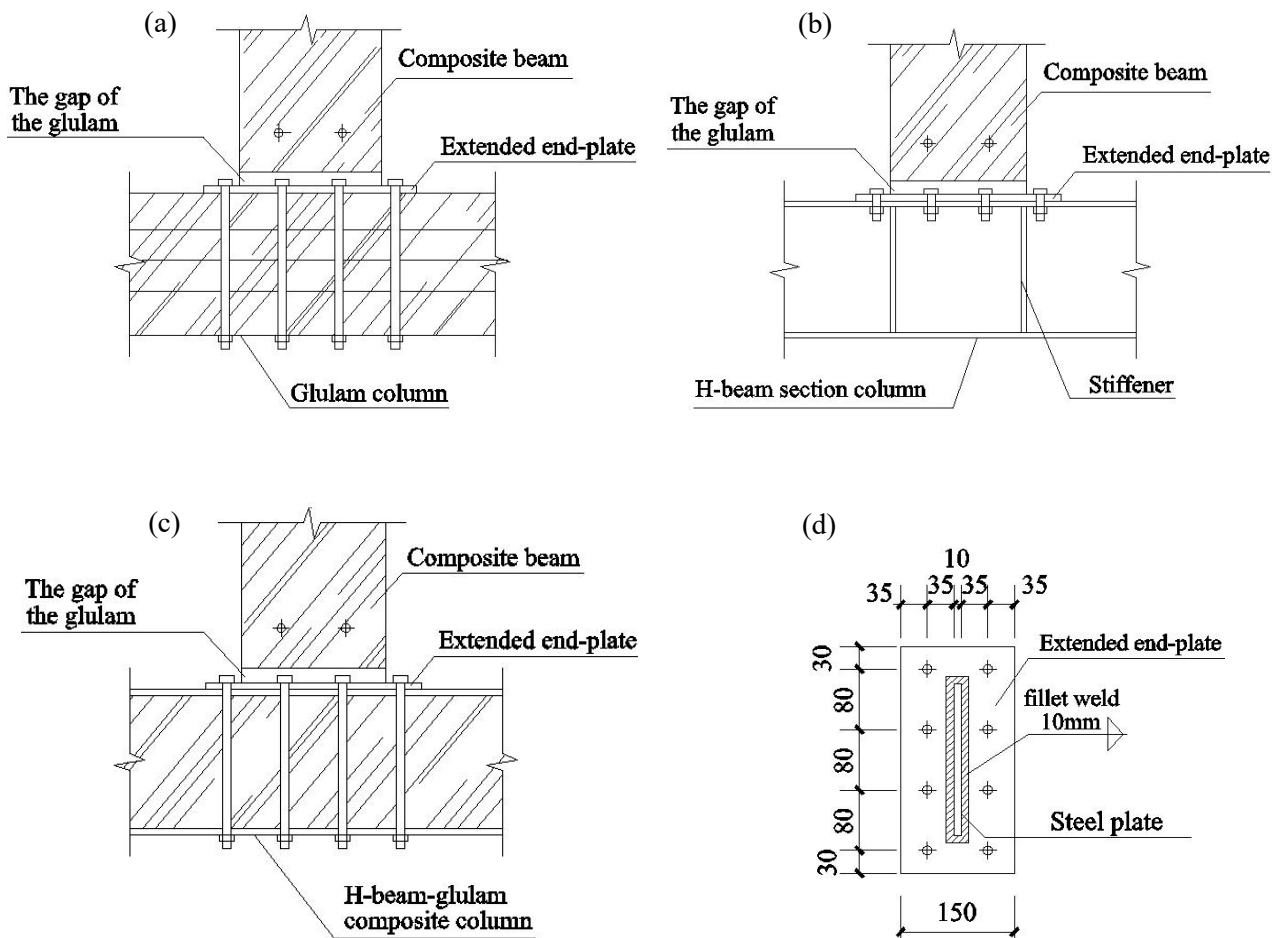


Fig.3. The diagram of each joint: (a)JT joint; (b)JS joint; (c)JSTC joint; (d)the bolt hole layout of the extended end-plate of each joint

## 2.2. MECHANICAL PROPERTIES OF MATERIALS

In the steel-glulam composite beam-to-column exterior joint test pieces, the glulam was glued from the same batch of larch boards. The steel plates and H-beams were produced by the same manufacturer, and the high-strength bolts used were the same batch of products. The fillet weld both used E43 welding rod, and the ultimately tensile strength of the fillet weld was 240MPa[7]. We did a test on the mechanical properties of wood and steel. The mechanical properties of timber and steel are shown in Table 1.

Table 1. Mechanical properties of timber and steel(MPa)

Materials	$E$	$\sigma$	$f_y$	$f_u$
Timber	12941	72.50	/	/
Steel	$2.03 \times 10^5$	/	260.41	399.88

Note. The values in the table both are the average of the material properties.  $E$  represents the elastic modulus ;  $\sigma$  represents the flexural strength of the timber;  $f_y$  represents the yield strength of the steel;  $f_u$  represents the ultimate strength of the steel.

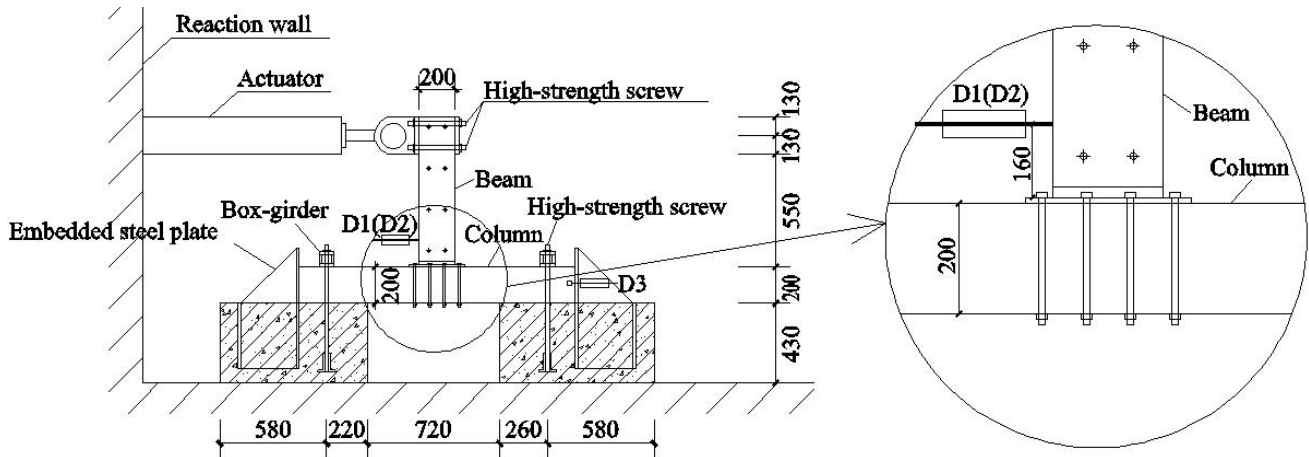
### 2.3. TEST DEVICE

The test was conducted in the structural test hall . The hall was equipped with a reaction wall and an electro-hydraulic servo loading system. Two concrete pedestals with embedded section steel were customized for the beam-to-column joint test. In order to facilitate loading, the column was placed horizontally on the concrete pedestal during the test. The left and right ends of the column were fixed to the pedestals by box-shaped steel beams and high-strength bolts. The composite beam was placed vertically, a horizontal load was applied to the end of the beam by an actuator. The displacement range of the horizontal actuator was  $\pm 250$ mm, and the load range was  $\pm 250$ kN. The arrangement of the displacement meter is shown in Fig.4. The magnetic table bases of the displacement meters D1 and D2 were directly adsorbed on the column surface. The edge of the magnetic table base was 160mm from the edge of the extended end-plate. The displacement measuring rod was parallel to the column axis and 260mm from the column axis. The relative rotation angles of beam-to-column joints were indirectly measured by the displacement meters D1 and D2. D1 and D2 were symmetrically arranged with the axis of the composite beam to check whether the composite beam was twisted under repeated loads. The displacement was automatically collected by the DH3821 dynamic strain test system, the frequency of data collection was 2 Hz.

### 2.4. LOADING PROTOCOL

The load-displacement data of the beam end in the test piece were automatically collected by the FTS electro-hydraulic servo loading system. The test loading was controlled by displacement.





(a) The diagram of test devices



(b) The photos of test devices

Fig.4. The test devices

Each stage of the cyclic loading was repeated twice. The displacement loading of each stage was increased by 3mm, and displacement loading was increased by 5mm when the amplitude was greater than 51mm. The loading speed was 0.5mm/s within the amplitude range of 0-30mm, and 1mm/s when the amplitude was greater than 30mm. When the peak value of the test load dropped below 85% of the ultimate load, the joint was regarded as failure and the loading was stopped.

### 3. TEST PHENOMENON AND ANALYSIS

The JT joint used glulam rectangular section column. When the displacement at the end of the beam was loaded to 15mm, the bolt on one side of the joint received a tensile force, and this tensile force was transmitted to the nut and the washer on the bottom of the timbered column through the screw.

The timber in the washer area was damaged by the compression stress, the washer was trapped in the timber, causing the outermost bolt to be pulled out slightly, and the end-plate was slightly lifted and bent, as shown in Fig.5(a). When the displacement was loaded to 33mm, the bending of the end-plate was large, the fillet weld cracked and the outermost bolt was obviously pulled out. The timber around the washer was further crushed, as shown in Fig.5(b). When the displacement was loaded to 61mm, about 3/4 of the end-plate was obviously lifted, the bolts were further pulled out, the timber at the washer was severely crushed, and the surface timber fibers fell off, as shown in Fig.5(c). At this time, the peak load at the end of the beam dropped below 85% of the ultimate load, and the joint had been damaged.

The JS joint was composed of H-beam column. At the initial loading period, the JS joint was in the elastic stage, and there was no obvious damage in the joint. When the load displacement at the end of the beam reached 6mm, initial micro-cracks appeared at one end of the fillet weld of extended end-plate, as shown in Fig.6(a). With the increase of the magnitude of the loading displacement, micro-cracks appeared at both ends of the fillet weld, the width and length of the crack were gradually increased. When the loading displacement was 21mm, the peak of test load decreased to less than 85% of the ultimate load, the joint was damaged, and the fillet weld cracking is shown in Fig.6(b). The cross section of the column at the JSTC joint was H-beam-glulam rectangular section. The test phenomenon of the JSTC joint was similar to the JS joint, the fillet welds at the end-plate were cracked, and the cracking of the fillet weld at the end-plate led to the ultimate failure, as shown in Fig.6(c-d). During the entire loading process of JS and JSTC joints, except for the fillet weld cracked at the end-plates, the other parts of the test specimens were not significantly damaged. The above test results show that the compressive strength of the timber in the column and the ultimately tensile strength of the fillet weld at the end-plate control the ultimately bearing capacity of the JT joint. For the JS and JSTC joints, the ultimately tensile strength of fillet welds at the extended end-plates controls their ultimately bearing capacity .



## 4. TEST PERFORMANCE PARAMETER ANALYSIS

### 4.1. HYSTERESIS CURVE

Under the low cyclic reversed loading, the P- $\Delta$  hysteresis curve at the end of the beam is shown in Fig.7(a-c). It can be seen that the central part of the hysteresis curve of the three beam-to-column exterior joints has different degrees of pinching, and the hysteresis loop develops from an initial shuttle shape to an inverse S-shape. Among them, because the JT joint used glulam columns and the initial slip between the bolt and the bolt hole was the largest, so the central pinching of the hysteresis loop was most obvious. The hysteresis loop of the JS joint was fuller than the JSTC joint.



Fig.5. Failure phenomenons of JT joint: (a)Failure phenomenon when the displacement was 15mm;(b)Failure phenomenon when the displacement was 33mm;(c)Failure phenomenon when the displacement was 61mm.

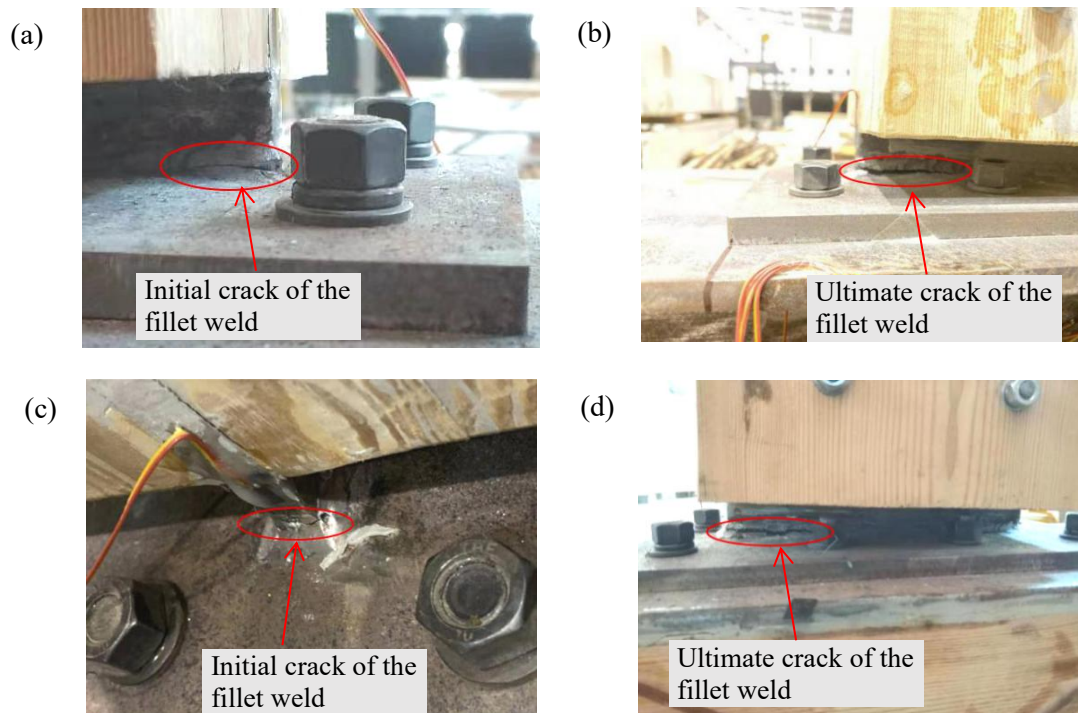


Fig.6. Failure phenomenons of JS joint and JSTC joint:(a)-(b) the crack of the fillet weld of JS joint;(c)-(d) the crack of the fillet weld of JSTC joint.

With the increase of the number of loading cycles, the hysteresis curves of the three exterior joints were gradually inclined to the displacement axis, this phenomena indicated that there was stiffness degradation at each joint.

## 4.2. SKELETON CURVE

The skeleton curve is the line connecting the peak points of the first cyclic load in each stage of the P- $\Delta$  hysteresis curve. The skeleton curves of the three joints are shown in Fig.7(d). It can be seen that:

- (1) The ultimate load of JT joint is about 23kN, JS joint is about 35kN and JSTC joint is about 34kN. These ultimate loads are the average values of the ultimate load values of each joint under forward and reverse loading. The ultimate bearing capacity of JT joint is the worst, and the ultimate bearing capacity of JS and JSTC joints are better and similar.
- (2) The skeleton curve of the JT joint has the smallest slope, which indicates that the joint composed of glulam column has the lowest stiffness. The stiffness of JS joint and JSTC joint are similar.

(3) Under the low cyclic reversed loading, the JS and JSTC joints have obvious yield points, and they experienced the phases of elasticity, yielding, and destruction. While the JT joint had no obvious yield point. The skeleton curves of JS and JSTC joints are basically coincident in the elastic phase.

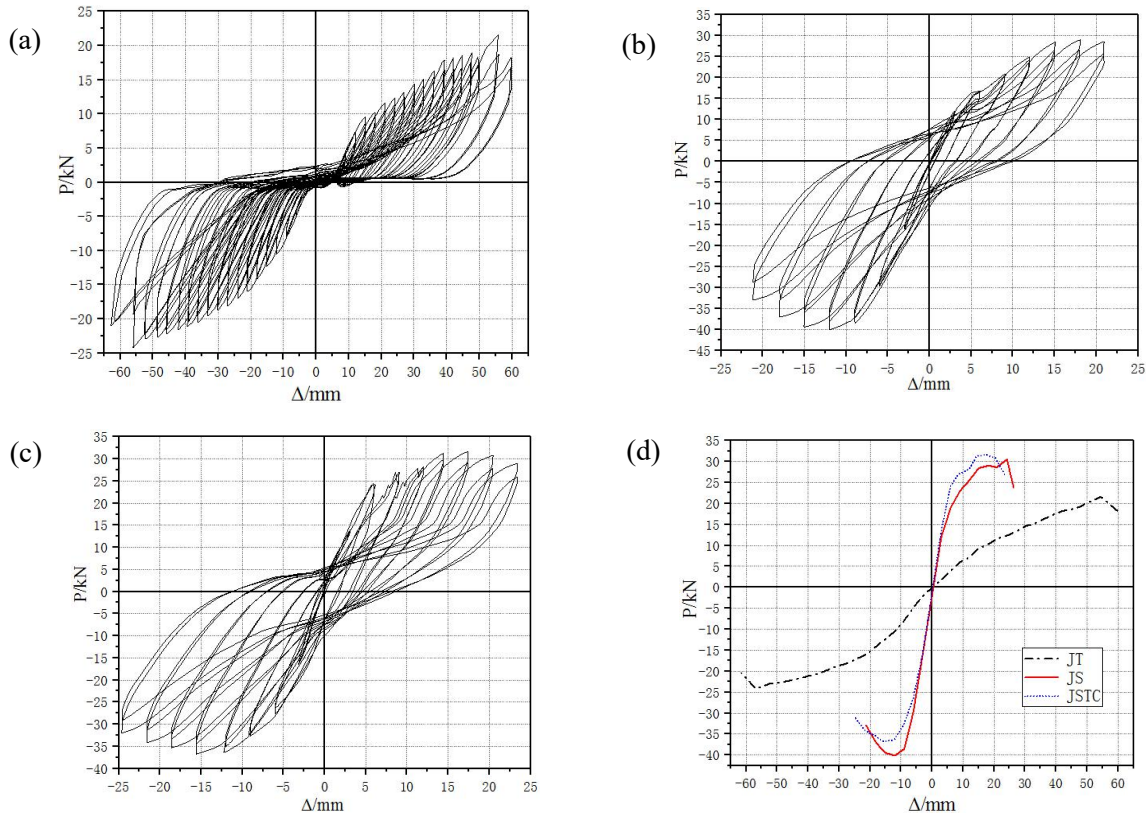


Fig.7. P-  $\Delta$  hysteretic curve and skeleton curve of each joint:(a)The P-  $\Delta$  hysteretic curve of JT joint; (b)The P-  $\Delta$  hysteretic curve of JS joint;(c)The P-  $\Delta$  hysteretic curve of JSTC joint;(d)The skeleton curve of each joint.

### 4.3. ENERGY DISSIPATION CAPACITY AND DUCTILITY COEFFICIENT

The energy dissipation capacity of a joint can be measured by the area surrounded by the hysteresis loop. We select the hysteresis loop where the ultimate load was located to calculate energy consumption. This paper use the energy dissipation coefficient  $E$  to evaluate the energy dissipation capacity of the steel-glulam composite beam-to-column joints[13]. The energy dissipation coefficient  $E$  is calculated according to the formula(4.1) and the calculation diagram is shown in Fig.8.

$$(4.1) \quad E = S_{(ABC+CDA)} / S_{(OBE+ODF)}$$

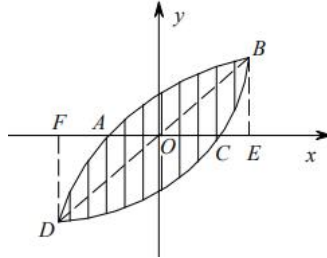


Fig.8. Calculation diagram of energy dissipation coefficient

The energy dissipation coefficients  $E$  of the three exterior joints are shown in Table 2. From Table 2, it can be seen that the energy dissipation coefficients of the JT and JSTC joints are 0.61 and 0.72, their energy dissipation capacities are relatively poor. By contrast, the energy dissipation coefficient of JS joint is 0.85, this shows that the joints composed of H-beam columns have a higher energy dissipation capacity.

Ductility coefficient reflects the deformation ability of a joint after it has entered the plastic state, that is an important index for evaluating the seismic performance of a joint. Ductility coefficient  $\mu = \Delta_u / \Delta_y$ , where:  $\Delta_u$  is the ultimate displacement;  $\Delta_y$  is the yield displacement [13]. From the skeleton curve, the yield points of JS and JSTC joints are obvious, and the inflection points on the skeleton curves can be used to determine the yield displacement and yield load. However, the JT joint has no obvious yield point, so the CEN method [5] recommended by the European Standardization Committee is used to determine the yield displacement and yield load of the joint. The ductility coefficient  $\mu$  is shown in Table 3. It can be seen that the ductility of the JS and JSTC joints is good, while the ductility of the JT joint is relatively poor.

Table 2. Main performance parameters of joints under cyclic loading

Specimen	yield point		extreme point		failure point		$\mu$	$E$
	$F_y$ (kN)	$\Delta_y$ (mm)	$P_{max}$ (kN)	$\Delta$ (mm)	$0.85P_{max}$ (kN)	$\Delta_u$ (mm)		
JT	19.62	40.87	22.90	55.66	19.47	60.60	1.48	0.61
JS	20.92	4.52	35.32	18.09	30.02	22.98	5.08	0.85
JSTC	25.28	6.00	34.22	16.49	29.09	24.22	4.04	0.72



Note: The data in the table are both the average values of each joint under forward and reverse loading.  $F_y$  represents the yield load;  $\Delta_y$  represents the yield displacement;  $P_{max}$  represents the ultimate load;  $\Delta$  represents the displacement corresponding to ultimate load;  $0.85P_{max}$  represents the failure load;  $\Delta_u$  represents the ultimate displacement;  $\mu$  represents the ductility coefficient;  $E$  represents the the energy dissipation coefficients.

## 5. CONCLUSION

Through pseudo-static test research of three steel-glulam composite beam-to-column exterior joints, the following conclusions can be obtained:

- (1) Under the low cyclic reversed loading, the JT joint did not show an obvious yield point during loading. When the JT joint was damaged, the timber at the washer area of the glulam column was crushed and the weld on the extended end-plate had cracked. The JS and JSTC joints had obvious yield points, and they experienced three stages of elasticity, yield and failure obviously. The size and strength of the weld on the extended end-plate controlled the ultimate load at the end of the beam.
- (2) The steel-glulam composite beam-to-column exterior joints connected by the extended end-plate and bolts had higher ultimate bearing capacity. And the ultimate bearing capacity of the JT joint composed of glulam column is the worst, that of the JS and JSTC joint are similar.
- (3) The energy dissipation capacity and ductility of the JT joint are the worst, the JSTC joint are better, and the JS joint are the best. The stiffness of JT joint is the lowest, that of JS and JSTC joints are similar.
- (4) In the steel-glulam composite beam-to-column exterior joints, the steel and glulam have better synergistic mechanical property. The seismic performance of JT joint composed of glulam column is the worst. And the seismic performance of JS joint composed of H-beam column with stiffeners is better than that of JSTC joint composed of H-beam-glulam composite column.

## ACKNOWLEDGMENTS

This study was supported by the National Science Foundation of China under Grant no.5127425 and the Scientific Innovation Fund for Post-graduates of Central South University of Forestry and

Technology. The experiment was supported by the Hunan Engineering Laboratory of Modern timber Structure Engineering Materials Manufacturing and Application Technology.

## REFERENCE

1. Bai RS and Jiang ZL. "On the research progress of composite structure of steel-timber ", *Journal of hebei university of architecture and engineering* 34(3):75-78,2016.
2. Bursi OS, Ferrario F, and Pucinotti R. "Seismic-induced fire analysis of steel-concrete composite beam-to-column joints:bolted solutions ", In: *International Conference on Composite Construction in Steel and Concrete 2008 Composite Construction in Steel and Concrete VI*(493-505),2008.
3. Chiniforush AA, Valipour H, and Akbarnezhad A. "Steel-timber composite (STC) beams: numerical simulation of long-term behaviour ", *Ce/papers* 1(2-3):2051–2059,2017.
4. Clouston P and Schreyer A. "Design and Use of timber–Concrete Composites ", *Practice periodical on structural design and construction*13(4):167-173(ASCE)1084-0680,2008.
5. EN 1995-1-1 Eurocode 5: design of timber structures:part 1-1: general common rules and rules for buildings, Brussels, Belgium: CEN,2004.
6. Fujita M and Iwata M. "Bending test of the composite steel-timber beam ", *Applied Mechanics and Materials* vol. 351-352, pp. 415-421,2013.
7. GB50017-2017. Standard for design of steel structures. Leeds: China building industry press, Beijing,2017.
8. Hassanieh A, Valipour HR, and Bradford MA. "Experimental and numerical study of steel-timber composite (STC) beams ", *Journal of Constructional Steel Research*, vol. 122, pp. 367–378,2016.
9. Hassanieh A, Valipour HR, and Bradford MA. "Experimental and analytical behaviour of steel-timber composite connections ", *Construction and Building Materials* vol. 118, pp. 63–75,2016.
10. Henrique Jorge JON and Francisco Miguel MO. "Glued Composite Timber-Concrete Beams.II: Analysis and Tests of Beam Specimens", *Journal of Structural Engineering*136(10):1246-1254,2010.
11. Hiroshi Kuramoto, Bing Li, and Kimreth Meas. "Experimental and Analytical Performance Evaluation of Engineering Wood Encased Concrete-Steel beam-to-column Joints" *Journal of Structural Engineering*137(8): 822-833,2011.
12. Jerzy J and Tomasz PN. "Solid timber beams strengthened with steel plates experimental studies ", *Construction and Building Materials* (63):81-88,2014.
13. JGJ/T101-2015, Specification for Seismic Test of Buildings. Leeds: China building industry press, Beijing,2015.
14. Jiang LZ, Qi JJ, and Zhou BW. "Lateral and Local Stability of Steel-Concrete Composite Beam ", *Advanced Materials Research* Vol.168-170, pp.721-729,2010.
15. Mohamed AS, Konstantinos DT, and Satoshi Y. "Comprehensive FE Study of the Hysteretic Behavior of Steel–Concrete Composite and Noncomposite RWS Beam-to-Column Connections ", *Journal of Structural Engineering*144(9):04018150(1-13),2018.
16. Nouri F, Bradford M, and Valipour H. "Steel-Timber Composite Beam-to-Column Connections with Shear Tab ", *Journal of structural engineering* 145(3):04018268:1-14,2019.
17. Tohid GG, Hui J, and Damien H. "Composite Timber Beams Strengthened by Steel and CFRP ", *Journal of Composite Construction* 21(1):04016059(1-11),2017.

18. Wang JR, Duan SW, and He JW. "Experimental Analysis of Eccentric Compression Performance of Larch timber-Steel Composite Columns ", *Advances in Civil Engineering* Vol. 2019 Article ID3102416, pp. 1-17,2019.
19. Wang XD and Chen ZH, "Research status and development prospect of steel-timber composite structure ", In: *Proceedings of the 2011 annual conference on steel structure Tianjin, China, October 2011*, pp.654-657,2019.
20. Yin YZ , Zhang Y. "Research On The Seismic Behavior Of Concrete-Filled Steel Tubular Column And Steel Beam Joint ", *Applied Mechanics and Materials* ISSN: 1662-7482, vol. 204-208, pp. 2528-2532,2012.
21. Zhang YZ, Raftery GM, and Quenneville P. "Experimental and Analytical Investigations of a Timber–Concrete Composite Beam Using a Hard timber Interface Layer ", *Journal of Structural Engineering* 145(7):04019052(1-15),2019.

### LIST OF FIGURES AND TABLES:

- Fig.1. Steel- timber composite beam:(a)section form of composite beam;(b)photo of composite beam
- Fig.2. Cross-section form of column in each joint:(a)JT joint ;(b)JS joint;(c)JSTC joint
- Fig.3. The diagram of each joint: (a)JT joint; (b)joint; (c)JSTC joint; (d)the bolt hole layout of the extended end-plate of each joint
- Fig.4. The test devices:(a)The diagram of test devices;(b)The photos of test devices
- Fig.5. Failure phenomenons of JT joint: (a)Failure phenomenon when the displacement was 15mm;(b)Failure phenomenon when the displacement was 33mm;(c)Failure phenomenon when the displacement was 61mm
- Fig.6. Failure phenomenons of JS joint and JSTC joint:(a)-(b) the crack of the fillet weld of JS joint;(c)-(d) the crack of the fillet weld of JSTC joint.
- Fig.7. P-  $\Delta$  hysteretic curve and skeleton curve of each joint:(a)JT joint; (b)JS joint;(c)JSTC joint;(d)The skeleton curve of each joint
- Fig.8. Calculation diagram of energy dissipation coefficient
- Table 1. Mechanical properties of timber and steel(MPa)
- Table 2. Main performance parameters of joints under cyclic loading



